Title
THE KINETICS AND THERMODYNAMICS OF DECOMPOSITION OF DOLOMITE IN VACUUM

Author
Knauf, Elizabeth Kridel.

Publication Date
1977-06-01

THE KINETICS AND THERMODYNAMICS OF DECOMPOSITION OF DOLOMITE IN VACUUM

Elizabeth Kridel Knauf
(M. S. thesis)

June 1977

Prepared for the U. S. Energy Research and Development Administration under Contract W-7405-ENG-48

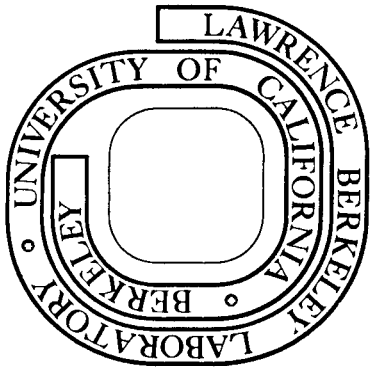

DISCLAIMER

THE KINETICS AND THERMODYNAMICS OF DECOMPOSITION OF DOLOMITE IN VACUUM

Contents

THE KINETICS AND THERMODYNAMICS OF DECOMPOSITION OF DOLOMITE IN VACUUM

Elizabeth Kridel Knauf

Materials and Molecular Research Division, Lawrence Berkeley Laboratory and Department of Materials Science and Mineral Engineering, University of California, Berkeley, California 94720

ABSTRACT

Torsion effusion and torsion Langmuir techniques were used to study the decomposition of dolomite in vacuum. Free surface decomposition from the $(10\bar{1}1)$ face of a dolomite single crystal by the reaction

$$CaMg(CO_3)_2 \rightarrow CaO + MgO + 2CO_2$$

had an apparent activation enthalpy of 46.5 Kcal, and the enthalpy for the equilibrium reaction, when corrected for an orifice size dependency, was 52.5 Kcal in the temperature range 750 - 900 °K. The apparent activation entropy for the reaction was 22.3 eu, which is less than the entropy of the equilibrium reaction, 47.6 eu. The ratio of the free surface decomposition pressure to the equilibrium pressure was 1.0×10^{-4} at 850°K.

INTRODUCTION

Dolomite, $CaMg(CO_3)_2$ decomposition has been studied extensively, mainly by differential thermal analysis techniques[1-6]. At low CO_2 pressures, dolomite decomposes by the reaction:

$$CaMg(CO_3)_2 \rightarrow CaO(s) + MgO(s) + CO_2(g)$$

At carbon dioxide back pressures greater than 50mm, the decomposition becomes a twostep process with the reaction:

$$CaMg(CO_3)_2 \rightarrow MgO(s) + CaCO_3(s) + CO_2(g)$$

occurring first and with $CaCO_3$ decomposition occurring at a higher temperature. As the back pressure is increased, the second decomposition endotherm, which corresponds to the calcite decomposition, is shifted to higher temperatures. The peak maximum moves from 795°C at 50mm CO_2 to 970°C at one atmosphere, while the endotherm peak for the magnesite decomposition remains at about 795°C unaffected by the CO_2 pressure. For this reason dolomite is used to calibrate atmospheric conditions in DTA experiments.[2]

Studies of dolomite decomposition at high temperatures and pressures were conducted by Harker and Tuttle[7] and by Mitchell[8], who decomposed samples in sealed containers and measured the product pressures by means of a pressure gauge. An automatically recording sorption balance was used by Britton et al.[9] to study the kinetics of isothermal decomposition of dolomite pellets in vacuum in the range 900-1000°K. The energy of activation of the decomposition varied from 49.4 to 55.6 Kcal per mole for the different dolomite specimens studied.

Decomposition of dolomite is used to produce many tons of refractory brick each year for use as furnace liners. The oxide mixture produced by dolomite decomposition under controlled conditions has been found to be an effective stack gas getter for SO_2.[10]

In view of the industrial importance of the reaction, its thermodynamics and kinetics should be fully established. But there have been few measurements of equilibrium CO_2 pressures produced in dolomite decomposition and kinetic studies of the vacuum decomposition of single crystals have never been made. In this study torsion effusion and torsion Langmuir methods are applied to determine dolomite decomposition pressures and its decomposition kinetics. Recent work in our laboratory on barium sulfate,[11] calcium carbonate,[12] and barium carbonate[13] has shown that these methods are ideally suited for the study of decomposition reactions.

Theoretical Background

The torsion effusion technique[14] is a method for measuring directly the recoil force of a vapor that effuses under Knudsen flow conditions into a vacuum from a small orifice in a cell containing the reactants. The observed pressure, P_{obs} will be the equilibrium pressure for the decomposition at that temperature, provided the rate at which gases escape through the orifice is much less than the rate at which gases can be generated by the decomposition reaction. This rate is dependent on the surface area of the sample, and its vaporization coefficient, α_v. If a step of the decomposition reaction is slow, the observed pressures will be less than the equilibrium pressures by amounts that depend on the orifice area. This area dependence is given by the Whitman-Motzfeld equation.[15,16]

$$P_{eq} = P_{obs}\left(1 + \frac{fa}{\alpha_v A}\right)$$

where a is the effusion orifice area, A is the effective vaporizing surface area, and f is the force correction factor for a nonideal orifice.[17,18]

In the torsion Langmuir method,[14] the pressure of gases which escape from a free surface into vacuum is measured. If all steps of the reaction are rapid compared to desorption, Langmuir and effusion pressures will be equal. However, if a step of the reaction is slow, the Langmuir pressure may be much lower than the effusion pressure and comparison of the two pressures as functions of temperature gives a measure of the irreversibility of the reaction.[19,20]

EXPERIMENTAL

The sample cells of 99.5% purity alumina are shown schematically in Fig. 1a and 1b. Two identical cells are placed in a graphite cell holder, with the orifices facing in opposite directions, as seen in Fig. 1c. Cells are protected from reaction with the graphite holder by molybdenum foil. The cell holder is pinned to an alumina support rod which extends out of the hot zone of the furnace. The rod is suspended by a Pt-Ni ribbon with dimensions .0127mm by .127mm. A mirror which is attached to the alumina rod is used to reflect a collimated light source through a window in the water cooled vacuum chamber onto a translucent scale mounted outside. The resistance furnace with tungsten heating elements is surrounded by a tantalum heat shield. Tantalum shields are placed above the furnace to prevent the torsion wire from being heated. The vacuum is maintained at 2×10^{-5} torr by an oil diffusion pump and a liquid nitrogen cold trap. The apparatus is shown schematically in Fig.2.

The recoil force of gases escaping from the cell orifice causes the torsion wire to twist, resulting in a deflection of the light beam on the scale. The entire suspension assembly is rotated by means of a gear system until the light beam is again centered evenly about the zero point on the scale. This rotation is measured by the numerical change of a counter coupled to the gearing system.

The vapor pressure of the decomposition reaction is then determined from

$$P = \frac{2\phi D}{q_1 a_1 f_1 + q_2 a_2 f_2}$$

where ϕ is the angle of rotation in radians, D is the torsion constant,

q is the moment arm of the orifice, a is the orifice area, and f is the force reduction factor.

Temperature measurements were made by a thermocouple placed below the suspended cell.

Experimental Preparation

A dolomite single crystal from Pomplona Spain was used for the Langmuir study. The material was ground to a fine powder for effusion measurements. A polycrystalline sample of Natividad dolomite, kindly provided by Kaiser Refractories, was used for additional effusion studies. The semi-quantitative spectrographic analysis by American Spectrographic Laboratories is shown in Table 1. All values are reported as the weight % oxides of the elements with Ca and Mg to the nearest 5%.

Table 1. Spectrographic Analysis of Dolomite Samples.

	Natividad Dolomite	Pamplona Dolomite
Mg	20. %	20. %
Ca	30.	35.
Si	0.2	0.03
Al	.05	.025
Fe	.07	.7
Pb	.015	<.003
Mm	.015	.08
Sr	.003	.04
Ba	<.001	.006
Cu	<.001	<.001
Ag	<.001	<.001
Na	<0.05	<0.05
K	<0.75	<0.75
Ni	<.001	<.001
Ti	.002	-
Zr	.01	-

For the effusion studies, crystals were ground to a fine powder with a mortar and pestle. Grinding for times on the order of hours has been shown to produce a decrease in temperature of the dolomite decomposition endotherm in DTA studies.[6] For this reason, crystals were ground for the minimum of time necessary to produce fine powder, about 1 minute for 10 grams of sample. Changes in X-ray spectra of the kind that were reported in the DTA study were not observed in this study, so it is unlikely that grinding produced changes in decomposition pressures.

X-ray diffraction patterns of the samples matched those for dolomite in the ASTM Powder Diffraction Files. The weight loss that resulted from complete decomposition of the Pamplona dolomite was found to be 48%, compared with the theoretical value of 47.7% for stoichiometric dolomite.

Langmuir samples were prepared by cleaving the crystal into slices approximately 1mm thick along the natural cleavage $(10\bar{1}1)$ planes. Sections were selected which had parallel faces. A crystal section was placed on the cell support disc, and the cell lid pressed tightly over it. Proper fit of the lid is vital in preventing leakage of gases from around the orifice edges. In many cases leakage did occur, as verified by visual observation of crystal decomposition in areas other than that defined by the orifice. In such cases data were discarded. At temperatures above 900°K, leakage occurred no matter how tight the fit. This fact greatly limited the temperature range of study. Slow heating to the experimental temperature was necessary to prevent the crystal from cracking due to its thermal shock.

System Calibration

Measurements of equilibrium effusion and free surface Langmuir decomposition pressures in a single apparatus minimizes the chance of obtaining experimental differences based on systematic equipment error. Extensive efforts were made to reduce systematic equipment error by proper calibration.

The furnace was calibrated by placing a dummy cell holder containing a thermocouple at a predetermined position in the furnace, a region where the cell temperature was constant to ±2°C over a distance of ±2 cm, and where the sample cell would be located during experimental runs. A reference thermocouple was placed 6mm below the cell. The temperature difference between the cell and the reference thermocouple was recorded as a function of temperature. Typically, the cell was 42-44° cooler in the experimental temperature range. The scatter in ΔT readings was 2°. The distance between the cell and reference thermocouple does not change during an experimental run, since the thermal expansion of the alumina rod is negligable ($\sim 10^{-4}$ mm). The platinum ribbon with the applied stress of the rod and loaded cell will expand elastically only about 5×10^{-3} cm.

The torsion constant of the ribbon was determined in the temperature range of study, while carrying approximately the same weight as during experimentation, this weight was a stainless steel disc with known moment of inertia. The period of oscillation for the system with the disc and for the system alone were measured. Periods were taken as the average time of several oscillations in order to minimize start and stop errors. The torsion constant which was obtained from

$$D = \frac{4\pi I_m}{t_{m+s}^2 - t_s^2}$$

was remeasured periodically during the course of experimentation, and found to vary less than 1.5%.

Cell orifice areas and moment arm lengths were measured with a comparitor. Several measurements were made for each orifice, and the results were averaged. Areas and lengths of effusion channels are summarized in Table 2.

Table 2. Effusion Geometries.

Cell	Hole diameter (1) cm	(2)	Channel Length (1) cm	(2)
Knudsen cell				
1	0.020	0.021	0.0800	0.0826
2	0.040	0.042	0.0839	0.0134
Langmuir cell				
3	0.2954	0.2954	0.0684	0.0792

The Torsion-effusion and Torsion Langmuir methods yield directly pressures as functions of temperature, but the level of systematic error in measurements is difficult to estimate. Accordingly, the vapor pressure and rates of vaporization of sodium chloride single crystal slices were measured and used for calibration. Sodium chloride has a vapor pressure of similar magnitude to the decomposition pressure of dolomite. The vaporization coefficient was carefully measured for NaCl by Ewing and Stern.[21] They report $\alpha_v = .74$ in our experimental range. But they find that increasing by a factor of 3 the surface area of material that vaporizes through a fixed projected area does not increase the flux. This result shows that actually $\alpha_v = 1$.[22]

Results for sodium chloride are given in Table 3, and shown graphically in Fig. 3. In this plot of log P vs. 1/T, by the second law method the slope yields the enthalpy for the reaction ΔH, and the y intercept determines the entropy ΔS, since

$$-\ln P = \frac{\Delta H}{RT} - \frac{\Delta S}{R}$$

where R is the gas constant. Measured enthalpies correspond quite closely to accepted JANAF values, but accepted total NaCl pressures are about 0.85 our measured pressures. For bismuth accepted pressures are about 0.70 times our measured values, as seen in Fig. 4. Accordingly, measured dolomite pressures were multiplied by a factor of 0.81 to correct for systematic calibration errors. The measured Langmuir pressures for NaCl are very close to the equilibrium pressures, verifying a vaporization coefficient of one, independent of temperature. This result indicates that heat input is sufficient to prevent undercooling even during free surface evaporation into vacuum. When dolomite was decomposed the rate did not decrease with time, which indicates the porous product did not significantly reduce thermal transport.

Table 3. NaCl Vaporization Data

Cell		Temperature (°K)	Pressure (atm)	Heat of Vaporization (Kcal)
effusion diameter				
0.02cm	1	947	2.80×10^{-5}	
	2	991	8.64×10^{-5}	
	3	1000	1.08×10^{-4}	
	4	978	5.90×10^{-5}	
	5	1016	1.74×10^{-4}	
	6	961	3.60×10^{-5}	51.6
0.04cm	1	930	1.22×10^{-5}	
	2	1001	8.76×10^{-5}	
	3	988	6.41×10^{-5}	51.8

Table 3. (Continued)

Cell		Temperature (°K)	Pressure (atm)	Heat of Vaporization (Kcal)
Langmuir diameter				
0.30cm	1	883	3.24×10^{-6}	
	2	866	1.82×10^{-6}	
	3	877	2.65×10^{-6}	
	4	903	6.80×10^{-6}	
	5	800	9.18×10^{-7}	51.8
			JANAF	51.8

Dolomite Results

Dolomite experimental results are reported in Table 4, with pressures corrected as determined by the calibration test. Effusion results as seen in Fig. 5 show an orifice size dependence. The extrapolarion for zero orifice area was obtained using the Whitman-Motzfeld equation. The following were the experimentally found values of ΔH and ΔS.

	ΔH (Kcal/mole)	ΔS(cal/deg-mole)
0.02cm dia.	52.9 ± 0.7	47.4 ± 0.8
0.04cm dia.	53.3 ± 0.6	45.9 ± 0.8
0.04cm dia. low Fe	50.8 ± 0.4	42.9 ± 0.5
0.04cm dia. combined	52.0 ± 0.5	44.2 ± 0.7
Motzfeld extrapolation	52.5 ± 1.3	47.6 ± 1.6
	ΔH^*	ΔS^*
0.30cm dia. Langmuir	46.5 ± 0.1	22.3 ± 1.4

The Motzfeld extrapolation at the midpoint of the temperature and the average slope of the .02cm dia. and combined .04cm dia. data were used to determine the equilibrium heats and entropies, and their standard deviations are the sum of the enthalpy deviations from which they were derived. The low iron sample is seen to vary slightly from the values for Pamplona dolomite with the same orifice area. At 850°K the ratio of the Langmuir pressure

to the equilibrium pressure gave a vaporization coefficient of 1.0×10^{-4}.

At the lower end of the temperature range at least one hour was required to attain a steady pressure reading, while at the upper end only a half hour was necessary. Points were taken by alternately raising and lowering temperature to the temperature for a given point, to reduce the chances of systematic error in pressure observations. Effusion measurements were corrected by the force correction factor for a nonideal orifice, but these factors were not used for the torsion Langmuir measurements: because the vaporization coefficient is low, the condensation coefficient of molecules returning to the surface after reflecting from a wall would also be low.

Table 4. Dolomite Vaporization Data

Orifice Diameter		Temperature (°K)	Pressure(Atm)
0.2mm			
Run 1	1	850	5.85×10^{-4}
	2	842	4.07×10^{-4}
	3	859	7.02×10^{-4}
Run 2	1	805	9.32×10^{-5}
	2	828	2.57×10^{-4}
	3	849	5.39×10^{-4}
	4	814	1.52×10^{-4}
	5	843	4.31×10^{-4}
	6	863	8.51×10^{-4}
	7	885	1.73×10^{-3}
	8	770	1.94×10^{-5}
	9	789	4.83×10^{-5}
	10	833	2.86×10^{-4}
	11	800	7.37×10^{-5}

Table 4. (Continued)

Orifice Diameter		Temperature (°K)	Pressure(Atm)
0.4mm			
Run 1	1	853	2.19×10^{-4}
Run 2	1	785	1.52×10^{-5}
	2	827	8.91×10^{-5}
	3	879	6.06×10^{-4}
	4	847	1.93×10^{-4}
	5	827	9.96×10^{-6}
0.4mm	1	753	4.25×10^{-6}
Natividad	2	821	6.85×10^{-5}
Dolomite	3	881	6.00×10^{-4}
	4	853	2.16×10^{-4}
	5	801	3.06×10^{-5}
3.0mm Langmuir			
Run 1	1	850	8.08×10^{-8}
	2	871	1.57×10^{-7}
	3	861	1.17×10^{-7}
	4	881	2.28×10^{-7}
	5	876	1.76×10^{-7}
	6	856	1.30×10^{-7}
Run 2	1	824	3.90×10^{-8}
	2	838	5.69×10^{-8}
	3	851	8.34×10^{-8}
	4	874	1.73×10^{-7}
	5	868	1.34×10^{-7}
	6	884	2.44×10^{-7}
	7	900	4.24×10^{-7}
	8	890	3.01×10^{-7}

SEM photographs of a fully decomposed crystal are shown in Fig. 6. The first shows the crystal cross section. In this can be seen the track of microcracks left by the advancing interface, shown in greater detail in the second photograph. At 10,000X a granular surface is apparent. No pores are visible even though the material is only 44% of theoretical density.

X-ray powder patterns obtained with CuKα radiation are presented in Fig. 7. The upper pattern shows the sharp peaks of the starting material, and the lower, for fully decomposed dolomite, shows broad CaO and MgO peaks. Centers of the fully crystalline oxide peaks are marked. Samples which had been decomposed about 50% showed only dolomite crystalline peaks, with no evidence of oxide products, despite the fact that X-ray diffraction analysis is sufficiently sensitive to detect cubic crystalline constituents in concentrations greater than about 5%. The BET surface area measured for the oxide products of fully decomposed dolomite was $20.8 m^2/g$.

DISCUSSION

Thermodynamic and kinetic values obtained in this study are similar to values previously found for $CaCO_3$, $BaCO_3$ and $BaSO_4$, by similar techniques,[11-13, 23] summarized below.

	$H°$Kcal/ mole	$S°$Kcal/ °-mole	H^*Kcal/ mole	S^*Kcal/ °-mole
$CaMg(CO_3)_2$	52.5	46.7	46.5	22.3
$CaCO_3$	40.2[23]	35.6[23]	49.0[13]	23.7[13 calculated]
$BaCO_3$	60.25	35.05	54.0	12.8
$BaSO_4$ (to $SO_2+1/2O_2$)	140.7	61.5	136.4	12.8

Except for $CaCO_3$, the apparent activation enthalpies are slightly less than the equilibrium enthalpy, and the apparent entropies are all much less than the equilibrium values.

The equilibrium enthalpy values obtained in this study were very similar to those of Britton et al.,[9] for isothermal decomposition in vacuum using weight loss techniques. Their results varied from 55.66 Kcal/mole to 49.9 with different dolomite samples, compared to 52.5 found in this study.

Dolomite decomposition pressures are very similar to those of calcite decomposition, while those for magnesite are about 5 orders of magnitude higher at 800°K.[23] From the three decomposition pressures, we calculate -21.4 Kcal at 800°K,[23] for the free energy of formation of dolomite from calcium and magnesium carbonates, compared to -2.6 Kcal at 873° K reported by Stout and Robie[24]. This discrepancy may be due to a computational error.

Dolomite has a calcite type trigonal structure with Mg and Ca ions occupying alternate layers in the lattice. It is formed by the dolomitization of limestone by magnesium - bearing solutions.[25] The cleavage system is $(10\bar{1}1)$ in a $MgCO_3$ - $CaCO_3$ solid solution, the dolomite phase width is about two percent in the temperature range of these experiments.[26] CaO and MgO have similar face centered cubic structures, with oxygens in cubic close packing and calcium or magnesium cations occupying octahedral positions. Their limits of solid solubility in each other in the temperature range of these experiments is about 1%.[27]

In dolomite decomposition, the solid product that is in equilibrium with the undecomposed carbonate phase is amorphous and may be a metastable solid solution of the two oxides because solid state diffusion rates of Mg^{++} and Ca^{++} ions at the temperatures of study must be low. Cunningham and Kumar have found the product crystallite size to remain constant at approximately 700A with isothermal decomposition through a temperature range of 640-800°C.[28] The free energy of formation calculated above for dolomite is more negative than the true value by the unknown free energy of formation of the metastable oxide product(s) of decomposition. Beruto and Searcy isolated the metastable product of calcite decomposition[29] and found its heat of formation to be +3 Kcal greater than that of the stable form of calcium oxide.[30]

The apparent volume of the product of complete decomposition of a dolomite crystal was unchanged from the volume of the original crystal. From the molar volumes of dolomite we calculate that the product has a porosity of 56%. Pores through the product oxide were not visible with SEM examination. This result shows that the pore size must be less than

0.1μm diameter, the limit of resolution with SEM.

Transport of gaseous product through the oxide barrier did not become rate limiting in the dolomite Langmuir experiments. Crystals could be decomposed very little (0.1mm) before cell leakage became sufficient to cause apparent decomposition rates to increase. Until then, rates were time independent.

In endothermic decomposition reactions, it is commonly assumed that the rate limiting step is a surface step in which the activated complex is the adsorbed solid or gaseous product.[31] Searcy and Beruto[19] recently showed, however, that when the decomposition flux in vacuum is lower than the flux effusing from a Knudsen cell, other steps may be rate limiting, such as diffusion of the solid or gaseous reaction component in the reactant phase, or transfer of the oxide product at the reaction-product interface. Furthermore, the rate may be reduced because the solid product of reaction is metastable.

For dolomite, because the apparent activation enthalpy of decomposition is less than the enthalpy of the equilibrium reaction, some step other than the final step of desorption of CO_2 must be rate limiting. The lower pressures observed in the free vaporization experiment could be a result of decomposition to a metastable solid product. However, if this were the sole cause of difference between free vaporization and equilibrium pressures, the apparent ΔH would be greater than the equilibrium ΔH, which is contrary to experimental results. If no step of the decomposition were slow, the apparent heat of activation should be more positive than the heat of the equilibrium reaction by the heat of formation of the metastable phase.[12] Here the apparent heat

of activation is more negative than the heat of decomposition. From the available data, it is not possible to make a more definite conclusion about the nature of the rate limiting process.

It has recently been shown that the dependence of decomposition rates on product gas pressure must depend on whether the slowest step of the process is one for the gaseous or the solid reaction product.[30] Accordingly, the effect of CO_2 pressure on the rate of dolomite decomposition should be further investigated.

ACKNOWLEDGEMENT

I would like to thank Professor Alan W. Searcy, my research advisor, for his guidance throughout this endeavor, and Dr. David Meschi for his magic hand in correcting equipment malfunction, as well as many helpful discussions. The staff of Building 62, Emery, Rich, Ed, Sandy, and Glenn, are gratefully acknowledged for their enthusiastic support. My thanks to all the people in Searcy's research group for making this an enjoyable experience, particularly Basu for introducing me to the ways of torsion effusion. Gary Knudsen for his B.E.T. measurements, and Rama Shukla for answering my many questions. Gay Brazil is much appreciated for her typing of this thesis. To Bob Powell I give a special 'thank you' for his weightloss measurements, and many learning discussions.

Work performed under the auspices of the U. S. Energy Research and Development Administration.

REFERENCES

1. R. A. Rowland and D. R. Lewis, Am. Min. 36, 80 (1951).

2. J. W. Smith, D. R. Johnson, and M. Muller-Vonmos, Thermochimica Acta 8, 45 (1974).

3. W. R. Bandi and G. Krapf, Thermochimica Acta 14, 221 (1976).

4. R. A. W. Haul and H. Heystek, Am. Min. 37, 166 (1952).

5. D. L. Graf, Am. Min. 37, 1 (1952).

6. W. F. Bradley, J. F. Burst, and D. L. Graf, Am. Min. 38, 207 (1953).

7. R. I. Harker and O. F. Tuttle, Am. J. of Sci., 253, 209 (1955).

8. A. E. Mitchell, Chem. Soc. London J. 123, 1055 (1923).

9. H. T. S. Britton, S. J. Gregg and G. W. Winsor, Trans. Faraday 48, 70 (1951).

10. E. P. O'Neill et al. (USEPA) US Patent Appl. 553, 119 26, Feb. 1975. 11 pps. Avail. NTIS.

11. P. Mohazzabi and A. W. Searcy, J. Chem. Soc., Faraday Trans. I, 72, 290 (1976).

12. D. Beruto and A. W. Searcy, J. Chem. Soc., Faraday Trans. I, 70, 2145 (1974).

13. T. K. Basu, M.S. Thesis, University of California, June 1974.

14. J. Margrave, ed. The Characterization of High Temperature Vapors, (Wiley, New York, 1970), Ch. 5,6.

15. K. Motzfeld, J. Phys. Chem., 59, 139 (1955).

16. A. W. Searcy, A. Buchler and D. Beruto, High Temp. Sci., 6, 64 (1974).

17. R. D. Freeman and A. W. Searcy, J. Chem. Phys. 22, 762 (1954).

18. D. A. Schulz and A. W. Searcy, J. Chem. Phys. 36, 3099 (1962).

19. A. W. Searcy and D. Beruto, J. of Phys. Chem., 78, 1298 (1974).

20. A. W. Searcy and D. Beruto, J. Phys. Chem., 80, 425 (1976).

21. C. T. Ewing and K. H. Stern, J. of Phys. Chem., 79, 2007 (1975).

22. A. W. Searcy, unpublished work.

23. K. H. Stern and E. L. Weise, High Temperature Properties and Decomposition of Inorganic Salts, Part 2. Carbonates. NSRDS-NB530, (1969).

24. J. W. Stout and R. A. Robie, J. Phys. Chem., 67, 2248 (1963).

25. L. G. Berry and B. Mason, Mineralogy (W. H. Freeman & Co., San Francisco, 1959).

26. R. I. Harker and O. F. Tuttle, Am. J. of Sci. 253, 274 (1955).

27. R. C. Doman, J. B. Barr, R. N. Nally and A. M. Alper, J. Am. Ceram. Soc., 46, 313 (1963).

28. P. T. Cunningham and R. Kumer, private communication.

29. D. Beruto and A. W. Searcy, Nature, 263, 221 (1976).

30. D. Beruto and A. W. Searcy, unpublished work.

31. D. A. Young, Decomposition of Solids, Pergomon Press, Oxford, 1966.

FIGURE CAPTIONS

Fig. 1. Torsion cells and holder.

Fig. 2. Schematic diagram of the torsion effusion apparatus.

Fig. 3. NaCl calibration.

Fig. 4. Bismith calibration.

Fig. 5. Dolomite results.

Fig. 6. SEM photographs of fully decomposed dolomite.

Fig. 7. Dolomite x-ray diffraction patterns.

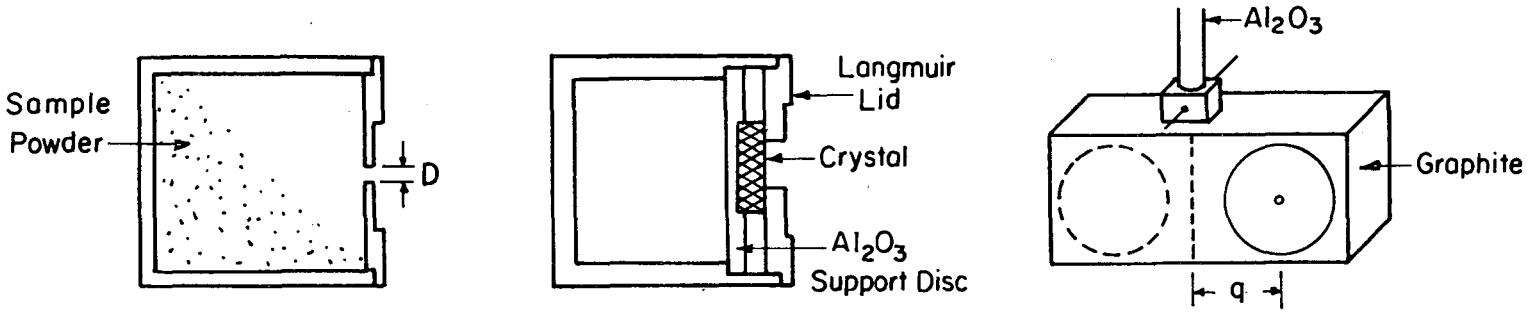
Sample
Powder
D
Langmuir
Lid
Crystal
Al_2O_3
Support Disc
Al_2O_3
Graphite
q
a. Effusion Cell
b. Langmuir Cell
c. Cell Holder
XBL775-5534

Fig. 1.

FIGURE CAPTIONS

Fig. 1. Torsion cells and holder.

Fig. 2. Schematic diagram of the torsion effusion apparatus.

Fig. 3. NaCl calibration.

Fig. 4. Bismith calibration.

Fig. 5. Dolomite results.

Fig. 6. SEM photographs of fully decomposed dolomite.

Fig. 7. Dolomite x-ray diffraction patterns.

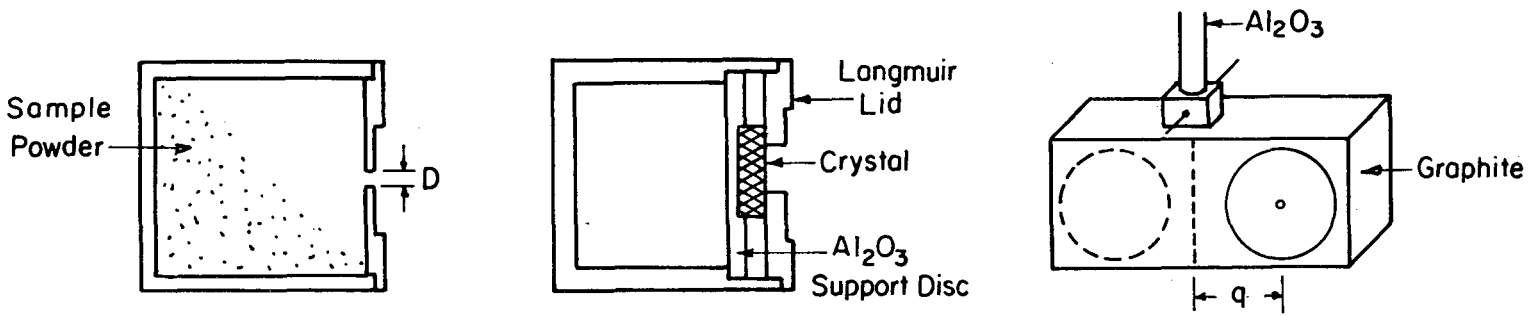

a. Effusion Cell b. Longmuir Cell c. Cell Holder

XBL775-5534

Fig. 1.

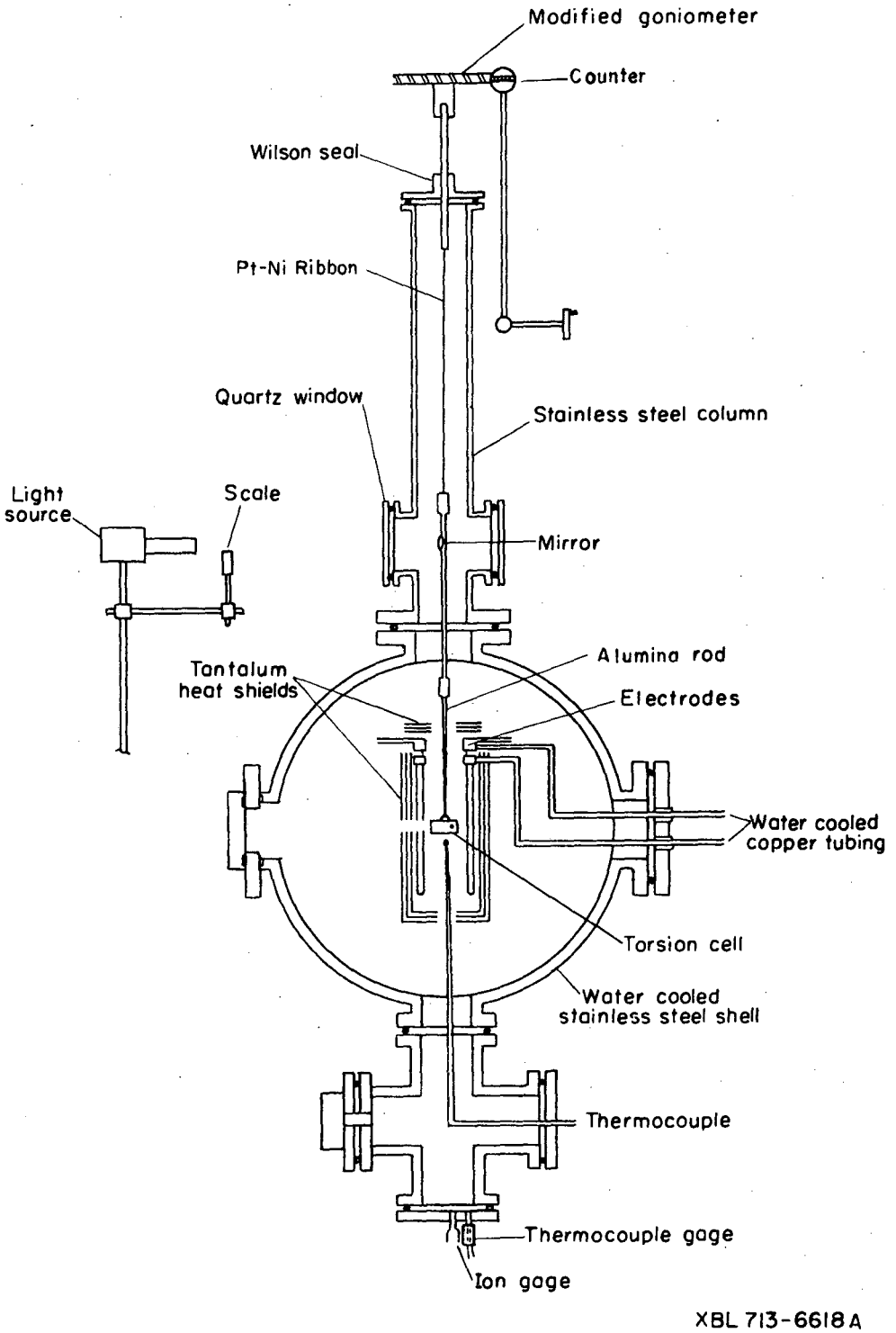

Fig. 2.

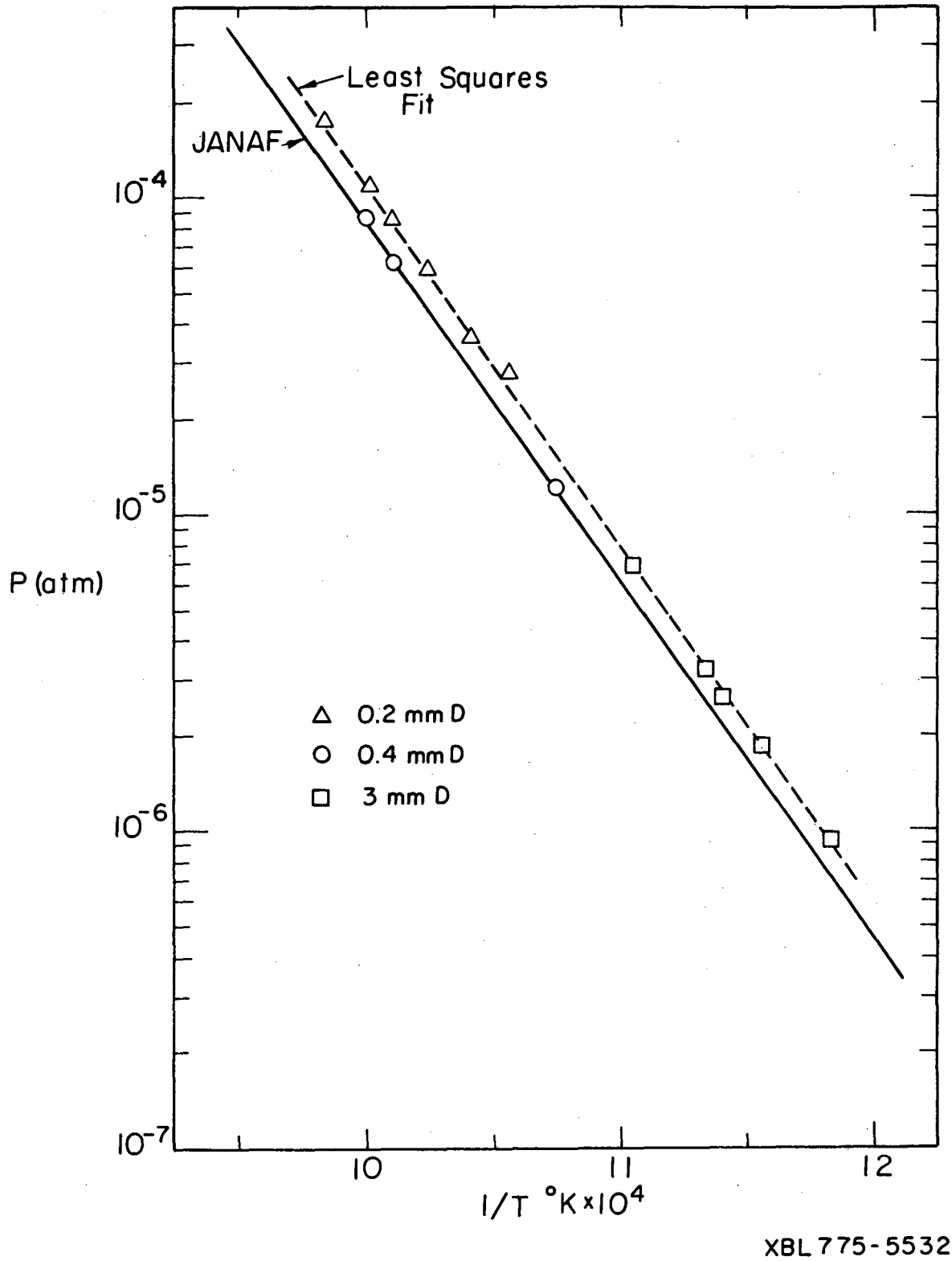
Least Squares Fit
JANAF
10^{-4}
10^{-5}
10^{-6}
10^{-7}
P (atm)
△ 0.2 mm D
○ 0.4 mm D
□ 3 mm D
10
11
12
1/T °K x 10^4
XBL 775-5532

Fig. 3.

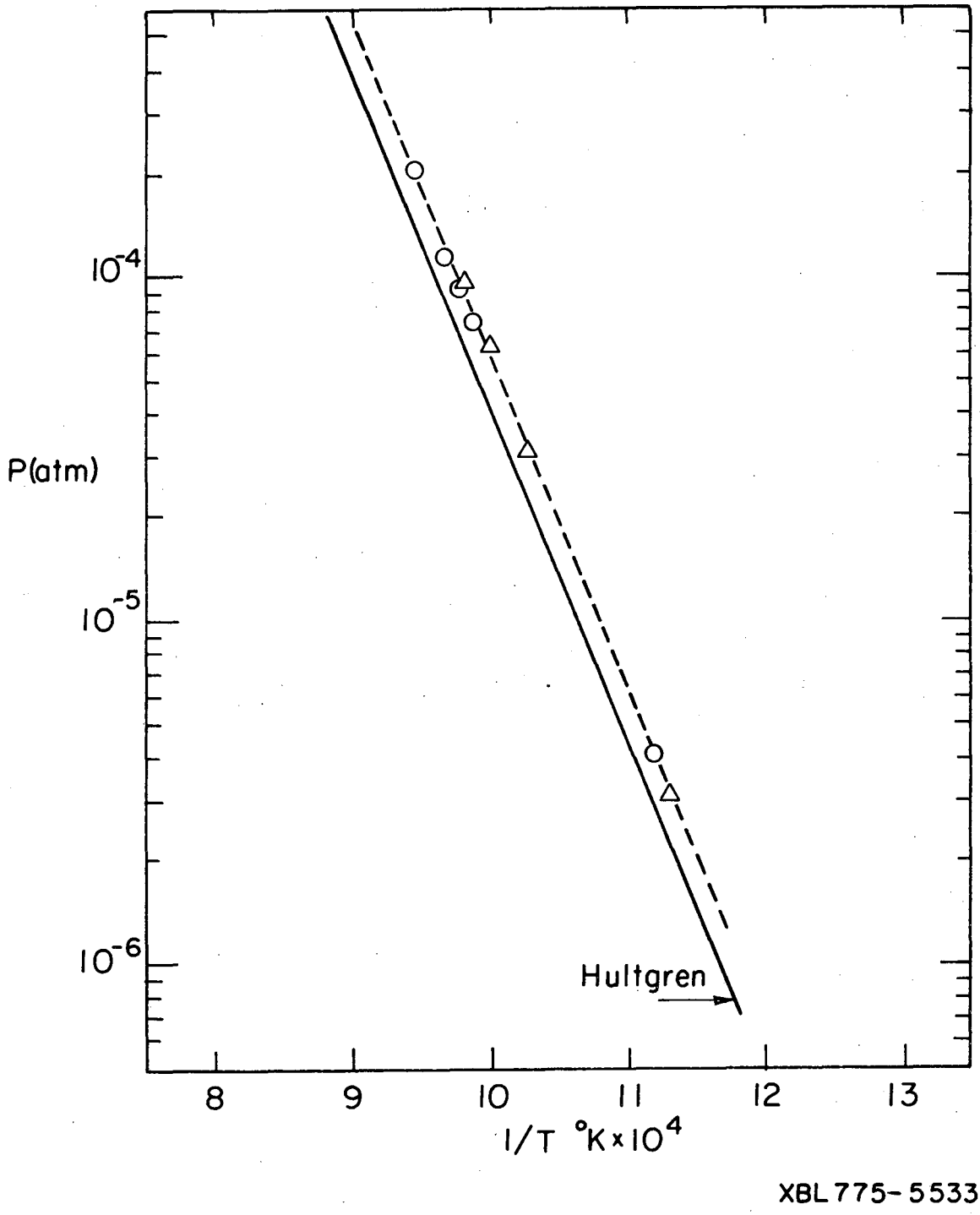

Fig. 4.

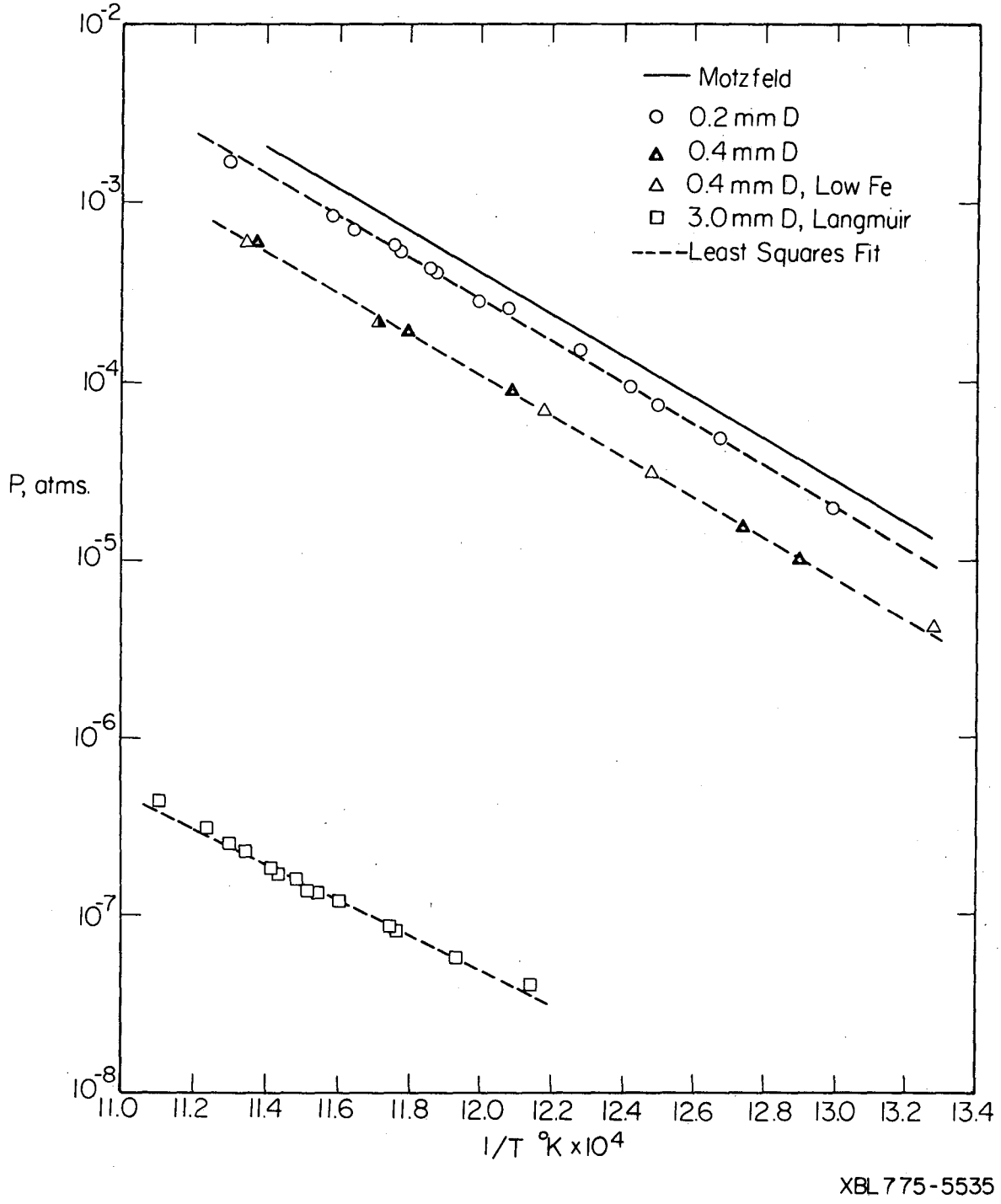
Motzfeld
0.2 mm D
0.4 mm D
0.4 mm D, Low Fe
3.0 mm D, Langmuir
Least Squares Fit
P, atms.
10^-2
10^-3
10^-4
10^-5
10^-6
10^-7
10^-8
11.0
11.2
11.4
11.6
11.8
12.0
12.2
12.4
12.6
12.8
13.0
13.2
13.4
1/T °K x10^4
XBL 775-5535

Fig. 5.

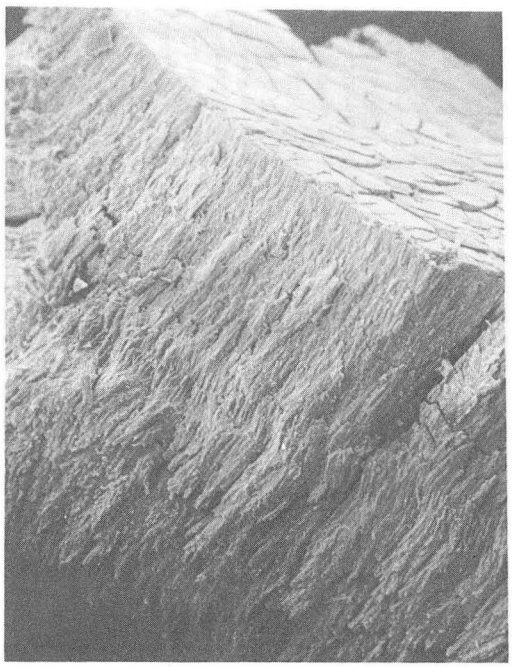

50 X

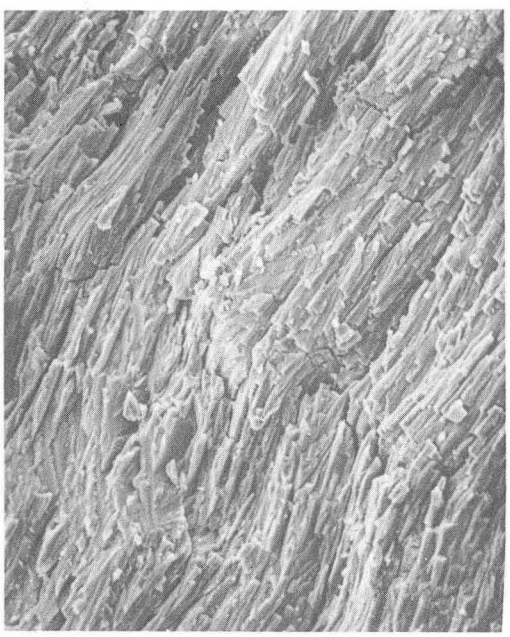

200X

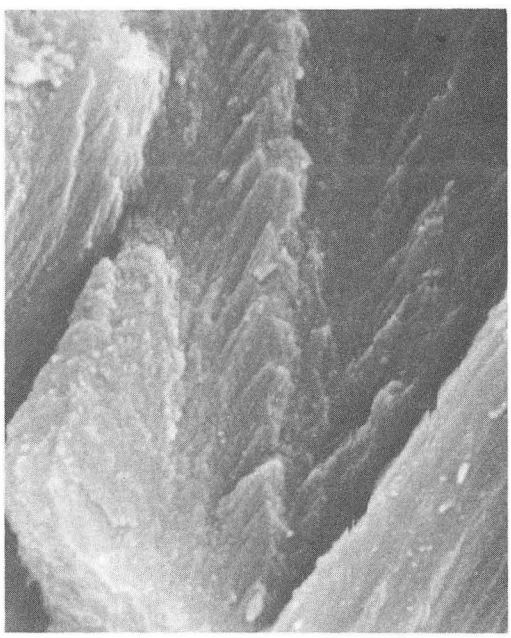

10,000X

XBB 776-5445

Fig. 6.

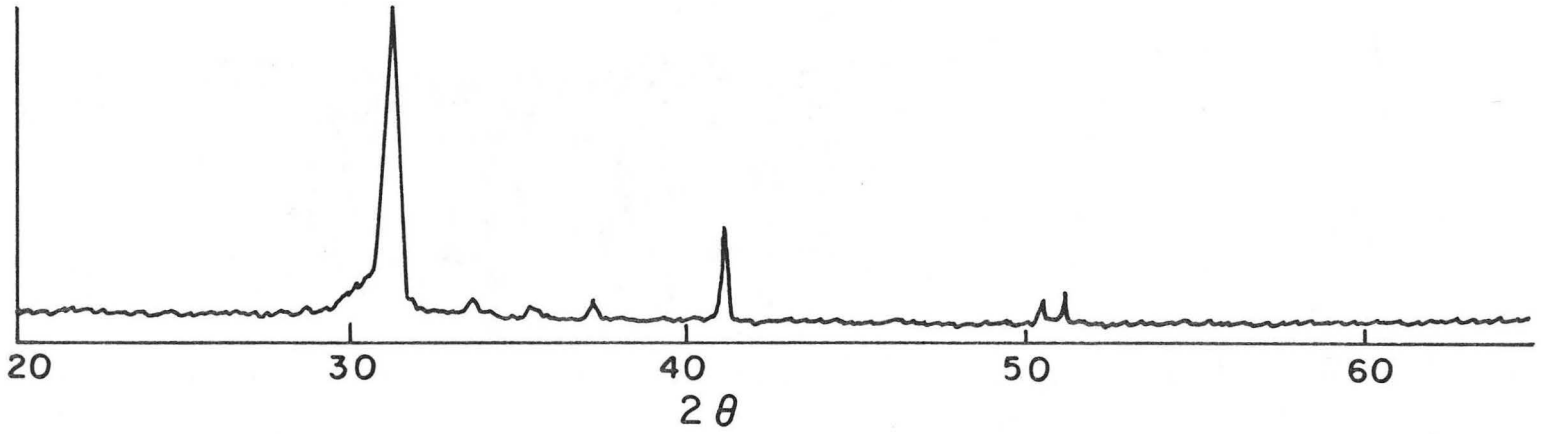

Pamplona Dolomite before Decomposition (TC =1000)

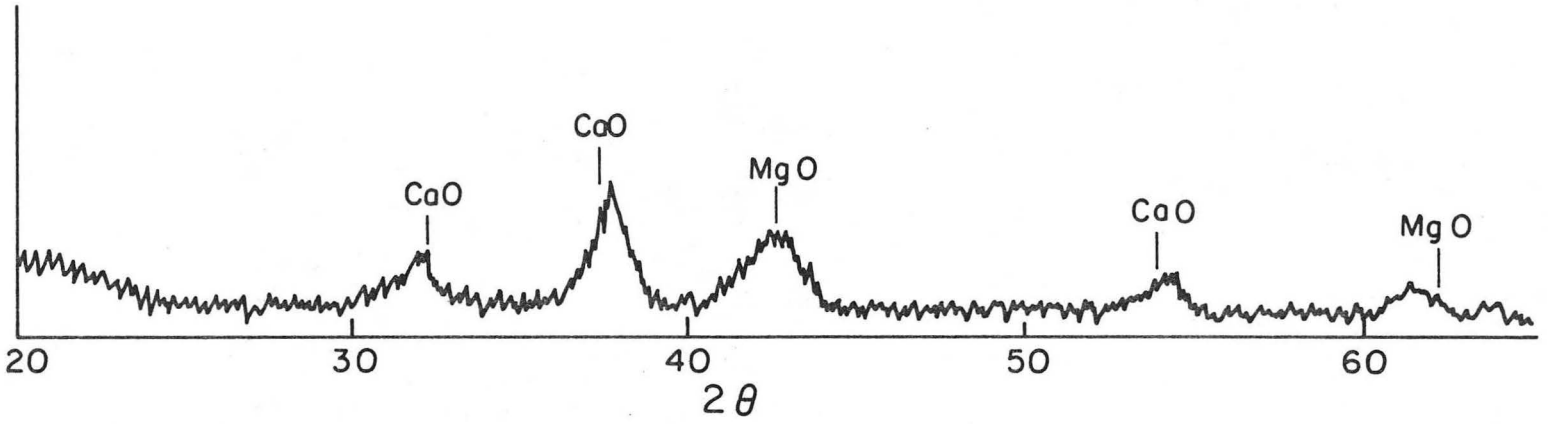

Fully Decomposed Powder, 580°C in Vacuum (TC=300)

XBL775-5531

Fig. 7.

TECHNICAL INFORMATION DIVISION
LAWRENCE BERKELEY LABORATORY
UNIVERSITY OF CALIFORNIA
BERKELEY, CALIFORNIA 94720